ELSEVIER

Journal of Power Sources 54 (1995) 120–126

JOURNAL OF POWER SOURCES

Electrochemical properties of cathodic materials synthesized by low-temperature techniques

Jean-Pierre Pereira-Ramos

Laboratoire d'Electrochimie, Catalyse et Synthèse Organique, C.N.R.S. UMR No. 28, 2 rue Henri-Dunant, 94320 Thiais, France

Abstract

After having introduced the definition of 'low temperature techniques', the electrochemical properties of various cathodic materials (oxides) for secondary lithium batteries are reported. The influence of the way of synthesis upon their electrochemical behaviour is examined and illustrated through several examples. A presentation of electrochemical results discussed in relation with the specific chemical, physical and structural properties emphasizes the significant advances afforded by these techniques (sol–gel processes, precipitation, ion-exchange redox reactions, etc.) in obtaining new high-performance cathodic materials for secondary lithium batteries. The most interesting results are obtained for the vanadium and manganese systems.

Keywords: Rechargeable cathodic materials; Cathodes; Low-temperature techniques

1. Introduction

In the 80s, besides the evaluation of well-known crystalline oxides, consistent attention has been devoted to novel types of rechargeable cathodic materials for Li batteries. Numerous new materials were studied to get the highest performance, i.e., especially a high rechargeability and cycle life: amorphous V_2O_5, V_2O_5–P_2O_5, MoO_3; non-stoichiometric compounds (V_6O_{13+x}, MoO_{3-x}), mixed oxides (Mo–V, W–V, Nb–V), bronzes (W, V). Nevertheless, no ideal intercalation compound was found among these materials which all have been synthesized through solid-state reactions at high temperature.

In fact, significant progress can still be made in the field of rechargeable cathodic materials when low-temperature techniques are applied to prepare solid phases. Low-temperature techniques require the formation or the treatment of a solid phase through a chemical or electrochemical reaction performed in a liquid phase (aqueous or organic medium) at moderate temperature (< 100 °C). Therefore, the low-temperature techniques cover numerous ways of preparations involving various chemical reactions such as precipitation, polymerization, hydrolysis, dehydration, redox, ion-exchange reactions or an electrochemical reaction performed in solution. Each of these processes or any combination of them constitutes a low-temperature technique for preparing Li intercalation materials usable in Li batteries [1].

In this work, we critically discuss the impact afforded by low-temperature techniques especially sol–gel synthesis and precipitation techniques on the electrochemical behaviour of the materials as prepared. In addition, to get further information on the interest of these ways of preparation, the results will be compared, when possible, with the properties of the closely related classical compounds. This paper includes three main parts related to different techniques: (i) sol–gel processes; (ii) precipitation reactions, and (iii) other techniques.

2. Discussion

2.1. Sol–gel processes

The sol–gel process offers new approaches to the synthesis of oxide materials. Starting from molecular precursors, an oxide network is obtained via inorganic polymerization reactions in solution. Compared with the conventional powder route, it offers many advantages such as a lower temperature processing or a better control of morphology and texture of materials. Moreover, the rheological properties of sol and gels allow

SSDI 0378-7753(94)02051-4

the fabrication of fibres or films by techniques such as spinning or dip-coating.

2.1.1. V_2O_5-based compounds

In this way, a wide variety of compounds are obtained: gel, xerogel, bronzes, and oxides. Their synthesis is described in Ref. [1]. The most important step is the preparation of the V_2O_5 xerogel obtained after removing almost all the water molecules from the corresponding gel at room temperature: the latter is prepared from inorganic precursors upon acidification of an aqueous solution of $NaVO_3$. V_2O_5 xerogel exhibits specific features. Indeed, due to its cationic exchange properties in aqueous solution, a wide variety of exchanged xerogels can be obtained. Thereafter, an appropriate heat treatment leads to various bronzes (M = Na, K, Ag) or mixed oxides (M = Fe, Al) depending on the nature of the cationic species.

V_2O_5 xerogel is composed of flat ribbons and characterized by a strong structural anisotropy corresponding to the stacking in the same direction of the V_2O_5 ribbons. Owing to its ionic and molecular exchange properties, pure thin films of V_2O_5 xerogel (VXG), 5 μm thick on platinum, can be used to undergo reversible Li insertion. In propylene carbonate (PC)-based electrolyte only about 0.2 H_2O is remaining in the host lattice. This kind of structural water removes at temperatures above 250 °C. While crystalline V_2O_5 is characterized by the existence of two well-shaped steps with a sharp voltage change at $x = 1$ F/mol, the potential interest of the VXG consists in having a single step for Li insertion centred around 3.1 V with a discharge capacity of nearly 250 Ah/kg, i.e., a faradaic yield of 1.8 F/mol corresponding to the quasi-quantitative reduction of V^{5+} ions to V^{4+} [1]. Two considerable increases in the partial molar entropy of Li, ΔS_{Li}, in VXG are evidenced for $0 < x < 0.1$ and $0.2 < x < 1.3$ and correlate well with X-ray diffraction (XRD) experiments which confirm the existence of two increasing turbostratic disordering processes inside the same composition ranges. During reduction, the first Li ions ($x < 0.2$) expel the PC molecules from the inter-ribbon spacing ($d = 21.6$ Å) leading to a collapsed host structure ($d = 10.6$ Å) in which subsequent Li accommodation occurs. Such important disordering processes combined with a poor electronic conductivity ($10^{-5}\ \Omega^{-1}\ cm^{-1}$) and a decrease of D_{Li} for high Li concentrations make that VXG must be rather considered with interest for practical use in microbatteries. Galvanostatic cycling experiments performed in the potential range from 3.8 to 2.5 V lead to a massic capacity of 80 Ah/kg after the 15th cycle. Such a result should be significantly improved by using a conducting additive like graphite or acetylene black.

The interest of the thin-film configuration, suitable for direct use in conventional Li cells has been applied in the case of amorphous $V_2O_5 \cdot 0.1H_2O$. This material obtained from dehydration of VXG at 230 °C was used in $LiCF_3SO_3$, poly(ethylene oxide) (PEO) electrolyte at 120 °C with an average cyclic efficiency during the first 46 cycles of 99% when insertion of 1.1 Li^+/V_2O_5 is involved in the potential interval from 3.5 to 2.2 V [2].

The sol–gel synthesis using organic precursors has been also applied. Single and mixed V_2O_5 and TiO_2 powders prepared by hydrolysis of the corresponding alkoxide precursors, then dried at 120 °C, and ball-milled together with acetylene black and $PEO/LiCF_3SO_3$ have been successfully used as a composite positive electrode at 120 °C [3]. Indeed to overcome the effect of structural and morphologic changes occurring in the composite electrode during Li insertion/extraction cycles increasing voids and number of isolated particles, the sol–gel technique allows to have a completely homogeneous material in which the oxide is microdispersed.

2.1.1.1. $M_xV_2O_5$ compounds

Investigation of sol–gel monoclinic bronzes (SGP) ($Na_{0.24}V_2O_5$, $Na_{0.33}V_2O_5$, $K_{0.25}V_2O_5$, $Ag_{0.33}V_2O_5$, $Ag_{0.4}V_2O_5$) illustrates the influence of the texture on the electrochemical performance of materials which behave as quasi-monocrystals from the point of view of the electrical and electrochemical properties [1]. The only difference between the SGP bronze and that prepared via solid–state reactions (SSR) is the size of their consistency domains, they are much higher for SGP bronze which probably promotes the rate of Li transport in this case. The sodium bronze consists of very long platelets of 1 to 2 μm wide all arranged parallel to the *ab*-plane, whereas packs of disordered particles of 2 to 10 μm are observed for the SSR bronze. The monoclinic structure of the sodium vanadium bronze synthesized via a SGP exhibits lattice parameters close to those of the SSR bronze. Nevertheless, XRD experiments reveal a high preferred orientation of the tunnel structure parallel to the *ab*-plane. In the same way, electronic conductivity of the SGP bronze is highly anisotropic with $\sigma_{\parallel} = 2\ \Omega^{-1}\ cm^{-1}$ and $\sigma_{\perp} = 2 \times 10^{-3}\ \Omega^{-1}\ cm^{-1}$ whereas $10^{-3}\ \Omega^{-1}\ cm^{-1}$ is found for SSR bronze. Whatever the SGP compound (Na, K, Ag), its electrochemical behaviour is generally characterized by three well-defined reversible insertion steps at average potentials of 3.3, 2.9 and 2.55 V within the composition range $0 < x \leqslant 0.33$–0.4, 0.35–$0.4 < x \leqslant 0.7$–0.75 and 0.7–$0.75 \leqslant x \leqslant 1.65$–$1.75$, respectively, is better than that of the corresponding SSR bronze, at least by a factor 2. Owing to its large consistency domains, it can be seen that improvement of the electronic conductivity of SGP material prevails on the active surface area available. Thus, high performance monoclinic V_2O_5 bronzes can be considered as rechargeable cathodic materials for Li batteries as shown in Fig. 1.

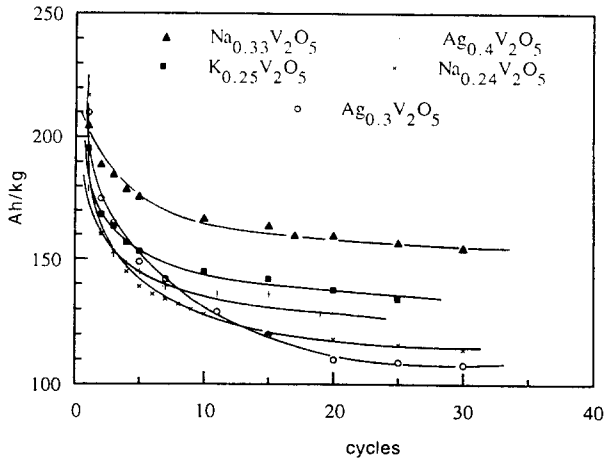

Fig. 1. Evolution of the specific capacity as a function of the number of cycles for various β-monoclinic $M_xV_2O_5$ bronzes prepared via a sol–gel process (1 M $LiClO_4$/PC; $C/6$ discharge/charge rate).

A new vanadium and iron oxide $Fe_{0.12}V_2O_{5.16}$ has been prepared using the same sol–gel procedure, previously described, but involving Fe^{3+} ions for the exchange reaction [4]. X-ray powder diagrams show cell parameters which resemble those of orthorhombic V_2O_5. Rietveld calculation allows to suggest the introduction of Fe^{3+} ions in sites located between four oxygen atoms of the V_2O_5 slabs with additional oxygen atoms along the c-axis, above and below the iron site to complete the iron octahedral environment [5]. Comparison of chronopotentiometric curves reported for the reduction of pure samples of V_2O_5 and $Fe_{0.12}V_2O_{5.16}$ highlights striking results: whereas the third reduction step expected for V_2O_5 does not appear, a significant well-shaped step is observed at 2.3 V and involves a faradaic yield of 0.8 F/mol of oxide. This behaviour could be reliable to a high value of electronic conductivity unlike the low conductivity encountered in LiV_2O_5. When a mixture of active material and graphite is used, four well-defined insertion processes appear in the potential window from 3.5 to 2 V. Current density in the range from 20 to 500 $\mu A/cm^2$ has little effect on the working voltage and the massic capacity, which indicates a high kinetics for the Li transport inside the compound ($\tilde{D}_{Li} = 10^{-10}$–$10^{-11}$ cm^2/s). Thus, a stable specific capacity around 300 Ah/kg is available.

This material provides an example of the effect of structural properties on the electrochemical behaviour since whatever the morphology, similar results are obtained. The presence of Fe^{3+} ions stabilizes the host structure as Li insertion proceeds: the Li composition ranges of the two-phase regions are narrower than for V_2O_5 while more extended one-phase regions are found, i.e., the emergence of new phases occurs for higher depths-of-discharge. All these features allow to achieve a good cycle life with a high massic capacity of 200 Ah/kg after the 40th cycle in the potential 3.8–2 V range ($C/4$).

2.1.2. MnO_2-based compounds

Reduction of an aqueous permanganate solution with fumaric acid ($C_4H_4O_4$) was used to synthesize MnO_2 oxides. For example, under these conditions gels are rapidly formed at room temperature in a molar ratio $KMnO_4/C_4H_4O_4 = 3$ in order to get a mean oxidation state of Mn, $z = 4$ in the gel. Drying and calcination of the gels lead to the formation of trivalent Mn in $Na_{0.7}MnO_2$ and $K_{0.25}MnO_2$, then transformed into MnO_2 by a sulfuric acid treatment [1]. Different forms of MnO_2 are obtained: λ-MnO_2, γ-MnO_2 (from an acid treatment at 90 °C) for $LiMnO_2$ and the birnessite $MnO_{1.84} \cdot 0.6H_2O$ for $Na_{0.7}MnO_2$ and $K_{0.25}MnO_2$. While results obtained with λ- and γ-MnO_2 are similar to those reported for the classical compounds, a novel and interesting behaviour is observed for the sol–gel birnessite.

The major advantage of the sol–gel birnessite consists in an unusual high depth-of-discharge/charge available for Li intercalation (0.9 F/Mn at 3 V), which makes this compound a promising rechargeable manganese dioxide. In this case, the type of crystallographic sites involved in Li accommodation, different from that found in the classical compound, mainly explains the improvement by a factor two (/classical) observed for electrochemical properties [6]. The $MnO_{1.85} \cdot 0.68H_2O$ obtained by the classical route has an hexagonal cell of C_dI_2-type and two consecutive layers generate an interlayer space with one trigonal antiprismatic (TAP) and two trigonal pyramidal (TPy) sites per manganese. Conservely, for the sol–gel compound, interlayer sites are trigonal prismatic in respect to the $Na_{0.7}MnO_2$ structure. Lithium easily enters trigonal prismatic sites (4.25–2.85 V) in a first step until to induce a monoclinic distortion for $x \approx 0.25$. From the value, further accommodation of Li ions occurs in the trigonal antiprismatic sites of monoclinic structure. Regarding the classical compound, Li-insertion process always occurs in trigonal antiprismatic sites of the initial hexagonal and the final monoclinic structure, the hexagonal to monoclinic distortion taking place only for a high Li content (0.5). The unusual presence of water molecules in the structure of this cathodic material for Li batteries does not prejudice to the rechargeability of the material since complete Li removal is observed without any important structural change and no significant water departure from the host lattice has been evidenced. Then, the elasticity necessary to sustain repeated Li insertion/extraction reactions seems to be provided by the interlayer water, which ensures the remarkable cycling behaviour of the material studied in flooded cells. During galvanostatic experiments within cycling limits from 4.2 to 2 V, the specific capacity slightly decreases from an

initial value of 200 Ah/kg (0.7/mol) to still about 150 Ah/kg by the 50th cycle. Another way to improve the cycle life would consist in maintaining some interlayer water and to have species able to limit the magnitude of the contraction/swelling process of the host structure induced by Li insertion/extraction. This point has been successfully considered with the use of interlayer Na and Bi ions (using precipitation reactions) ensuring the role of pillaring species, Fig. 2 [1,7].

The spinel $LiMn_2O_4$ has been synthesized via a sol–gel process followed by a heat treatment at a temperature of 300 °C determined to be the lowest temperature at which this phase can be synthesized [8]. Bulk samples are prepared in the temperature range from 300 to 800 °C. At temperature as low as 300 °C, grain size ranging from $\leqslant 0.03$ to 0.1 μm is obtained while 0.1 to 3 μm particles are observed when $LiMn_2O_4$ is prepared at 800 °C. The 300 °C sample has a lower capacity and larger polarization in the 4.5–3.5 V range but the highest capacity and the best cycling behaviour in the range from 3.5 to 2.2 V. The versatility of this solution technique using the acetate precursor route has been illustrated by an extension to the synthesis of $Na_xMn_2O_4$ compounds and layered $LiCoO_2$ [8].

2.2. Precipitation techniques

As part of an attempt to overcome the inherent limitations of the crystalline materials a growing interest in non-crystalline cathodes was noticed in the second half of the 80s. The precipitation technique seems to constitute a simple tool for preparing, at or near room temperature, amorphous cathodes of well-defined stoichiometry, or compounds with a low crystallinity.

2.2.1. Alkaline medium

A significant example is provided by the preparation of LiV_3O_8 [1]. Precipitation takes place after a dissolution-reaction sequence in the case of the preparation of LiV_3O_8 which is a promising rechargeable cathodic material:

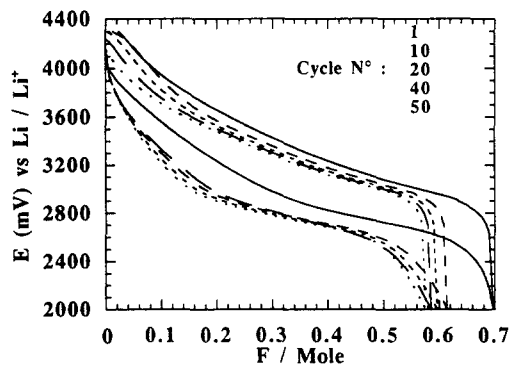

Fig. 2. Cycling properties of $Bi_{0.105}MnO_{2.11}\cdot 0.9H_2O$; 1 M $LiClO_4$/PC; 200 μA/cm²; from Ref. [7].

$$2LiOH + 3V_2O_5 \longrightarrow 2LiV_3O_8{}^{1} + H_2O \quad (1)$$

This reaction occurs by just dissolving in the alkaline solution (at 20 to 50 °C) the appropriate amount of V_2O_5. In 1 to 2 days, a red-brown disperse precipitate of the compound is formed, which proves completely amorphous at the X-ray analysis.

In this way, amorphous $Li_{1+x}V_3O_5$ and $Na_{1+x}V_3O_8$ of low crystallinity are obtained [1]. In comparison with well-crystallized cathodes, the compositional variations of the open-circuit voltages (OCV) for both materials have sloping curves with gradual changes versus x. These poorly crystalline cathodes do not show evidence of Li^+ ordering in given composition ranges and of constant repulsion forces among neighbours. Another important advantage provided by the low-temperature (LT) forms is their high surface area. For instance, LT $Na_{1+x}V_3O_8$ is formed of small needle-like crystals of 0.5 μm × 0.07 μm which results in a BET surface area of 40 m²/g against a surface area <1 m²/g for the high-temperature (HT) material. Such a disperse macrostructure will improve the rate capability and cycleability. Amorphous $Li_{1+x}V_3O_8$ and LT $Na_{1+x}V_3O_8$ can indeed intercalate up to 9 Li^+ in the unit cell, against a maximum of 6 for c-$Li_{1+x}V_3O_8$ and c-$Na_{1+x}V_3O_8$. Tested in Li cells simulating practical coin cells [9,10] they outperform the high temperature analogs, especially when high rates are used (Fig. 3). Composite cathode films based on LT $Na_{1+x}V_3O_8$ can be long cycled with minimal losses if the proper voltage range is chosen. Lamellar monoclinic vanadates like KV_3O_8, RbV_3O_8 and CsV_3O_8 have also been prepared with the same precipitation technique but these latter exhibit low capacities, low voltages and reduced cycleability [1].

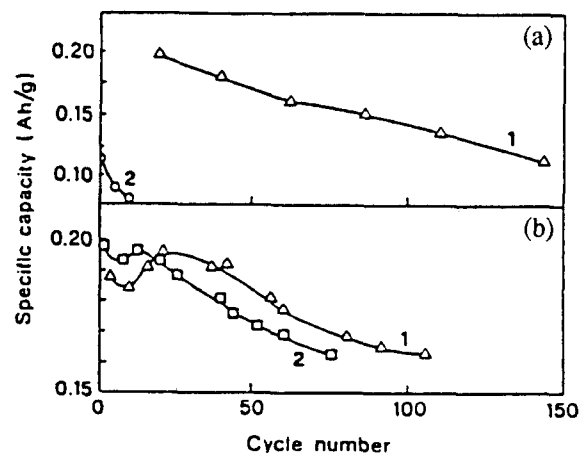

Fig. 3. (a) Cycling of cells containing (1) LT $Na_{1+x}V_3O_8$, and (2) HT $Na_{1+x}V_3O_8$. (b) Cycling of cells containing (1) LT $Na_{1+x}V_3O_8$, and (2) amorphous $Li_{1+x}V_3O_8$. $I_d = I_c = 1$ mA/cm²; from Ref. [10].

[1] This material is always obtained with a slight Li excess.

Co-precipitation reactions can be applied to the synthesis of new cation-deficient Mn–Co spinel oxides. $Mn_yCo_zO_4$ ($2.50 \leqslant (y+z) \leqslant 2.62$). Recent work has evidenced the interest of using the carbonate precursor method to obtain ultrafine materials and the simultaneous presence of valences (+4) and (+3) of Mn ions. Mixed Mn–Co carbonates are prepared from the addition of a $NaHCO_3$ solution to an aqueous solution of metallic cations(II) in the desired proportions under a continuous flow of CO_2. A subsequent heat treatment at 400 °C leads to cation-deficient mixed spinel oxides. Chronopotentiometric measurements show one main insertion process located near 2.8 V involving a faradaic yield of 0.7–0.8 F/mol of oxide while structural experiments do not reveal any alteration of the initial host lattice [11]. Owing to numerous cation vacancies, the magnitude of the Jahn–Teller effect is then reduced and the kinetics of Li^+ transport is proved to be high. Cycling galvanostatic experiments in the potential window from 4.0 to 1.6 V show an excellent capacity retention of 85 Ah/kg after 10 cycles (80–90%) for the tetragonal $Mn_{2.15}Co_{0.37}O_4$ and the cubic $Mn_{0.93}Co_{1.69}O_4$ phases.

A high voltage cathode material like $LiCoO_2$ can be prepared by a precipitation technique [12]. A lithium and ammonium hydroxyde solution is mixed to a Co(II) solution. The mixture is slowly evaporated at 60 °C under vacuum and the precipitate recovered is dried at 130 °C for 15 h. An appropriate heat treatment at 400 °C for 2 h leads to the $LiCoO_2$ formation. In comparison with the classical high temperature oxide usually obtained, X-ray diffraction experiments reveal the presence of slightly broader peaks which can be indexed on the basis of an hexagonal structure ($a = 2.83$ Å; $c = 13.90$ Å). Low-temperature LT $LiCoO_2$ exhibits a striking feature: its working voltage is around 3.7 V during the charge process against 3.9 V for the HT form while Li insertion occurs near 3.5 V. A rechargeable capacity of about 0.35 F/Co is available in the potential range from 3.9 to 3.4 V. Although this lower voltage could prevent decomposition of the organic electrolytes used in Li batteries, the cycle life of LT $LiCoO_2$ is lower than that of HT $LiCoO_2$. Due to the notable difference found in the electrochemical behaviour of LT and HT $LiCoO_2$ compounds, the question arises about how the ordering of Li and Co ions in particular sites of the host structure affects the electrochemical reactivity of $LiCoO_2$.

2.2.2. Acidification reactions

Well-crystallized layered $LiCoO_2$ can be also synthesized by organic acid methods [13]. For example, a solution containing cobalt nitrate, lithium hydroxyde and oxalic acid is adjusted to pH 4.6 with aqueous ammonia. The mixture is then evaporated (60–150 °C) and a cobalt complex precipitates. Further grinding and heating up to 900 °C lead to layered $LiCoO_2$. Other complexing agents like succinic, malic or tartaric acids can be used. The authors report that $LiCoO_2$ prepared by this new method shows lower polarization and higher capacity (120 Ah/kg) than that obtained by the conventional method (90–95 Ah/kg) with an attractive cycling behaviour when used between 4.3 and 3.7 V.

Tungsten and molybdenum trioxide hydrates have been synthesized through acidification by strong acids from a tungstate or molybdate solution Na_2MO_4 (M = W, Mo) and different phases occur, depending on the precipitation conditions [1]. Thus, in addition to $MO_3 \cdot nH_2O$ ($n = 1, 2$), where M = W or Mo, several tungstic or molybdic C-related acid phases (related to $WO_3 \cdot 0.5H_2O$ for W) containing small amounts of cations $x(A_2O)WO_3 \cdot yH_2O$ ($A = Li^+$, Na^+, K^+, NH_4^+; $x = 0.05$–1.3; $y = 0.5$–1) and $x[(NH_4)_2O]MoO_3 \cdot yH_2O$ ($x = 0.075$–0.042; $y = 0.4$–0.043) can be obtained. Although the layered structures of H_2WO_4, $H_2WO_4 \cdot H_2O$ and the tungstic acid C-phase provide a similar and unusual high discharge capacity equal to about 1.5 F/W (= 150 Ah/kg) compared with that usually achieved with conventional monoclinic WO_3(0.4–0.6 F/W) in the potential range from 3.2 to 1.8 V, poor cycling properties were achieved. As for W materials, the recharge efficiencies for the corresponding molybdenum oxide-based compounds never exceed 50%.

In order to overcome the unstability of all these interesting materials, moderate heat treatment has been considered over a wide temperature range. For instance, a high discharge capacity and a good cycle life have been reported for the hexagonal-type oxide $(xA_2O)WO_3$ ($A = Na^+$, K^+, NH_4^+; $x = 0.05$–0.14). Removing water molecules from the host lattice of the corresponding tungstic acid C-phase was ensured by a moderate heat treatment at 350 °C in air. High discharge capacities corresponding to a maximum Li uptake of 2 Li^+/W are reached in the potential 3–1 V range with a recharge efficiency of 75% [14].

Electrochemical performances of WO_3 resulting from the heat treatment of H_2WO_4 clearly show how much the intercalation of Li in the material depends on how the WO_3 host is made [1]. For $T = 250$, 500, 700 °C, monoclinic WO_3 is obtained with a degree of crystallinity and particle size depending on the heating temperature. Both the faradaic yield for a cutoff voltage of 2 V (0.6–0.8 F/W) and the charge/discharge efficiency (> 90%) are seen to be significantly improved for the LT-treated form (250 °C). The lowest degree of crystallinity and the higher surface area induced (25 m^2/g against 3–8 m^2/g for HT forms) under these conditions allow to achieve a high kinetics of Li transport in the structure ($\tilde{D}_{Li} = 10^{-11}$ cm^2/s) ensuring the best cycle life found for a crystalline monoclinic WO_3 ($\Delta x = 0.6$ after the 65th cycle; 3.8–2 V).

2.3. Other techniques

2.3.1. Chemical oxidative reactions

High-performance porous molybdenum oxides can be synthesized by oxidation of MoO_3 powder with H_2O_2 solution at 60 °C [15]. After evaporation of the resulting solution depending on the thermal decomposition conditions, carried out at 170 or 400 °C in air and at 200 °C under vacuum, MoO_3 oxides with different degree of crystallinity are obtained. Amorphous MoO_3 can be prepared by using a closely related procedure. During the MoO_3 treatment with H_2O_2, MoO_3 would intercalate oxygen in the layers, and the oxygen liberated by heating would give porous oxides. An excellent discharge capacity of 400 Ah/kg is achieved, twice the usual crystalline oxide one with the two well-known insertion steps. The recharge efficiency in the first cycle is nearly 75%, but no additional result on their cycle life is available.

Considerable improvement of the rechargeability of LT $LiCo_{0.9}Ni_{0.1}O_2$ (400 °C) is obtained by leaching some Li and a small amount of Co by acid treatment [16]. In this way, a defect spinel phase $Li_{0.4}Co_{0.8}Ni_{0.1}O_2$ is obtained which is significantly more stable to Li insertion/extraction reactions than the parent quasi-spinel phase. When cycling experiments are performed in the potential range from 4.2 to 2.5 V with mean voltage values of 3.4 and 3.6 V for the reduction/oxidation processes, a high capacity of 100 Ah/kg is reached after four cycles. This kind of synthesis is promising to increase the rechargeable capacity and stability of LT $Li[Co_{2-z}Ni_z]O_4$ $(0<z<2)$.

High-performance vanadium bronzes $M_yV_2O_5$ (M = Cu, Ag) have been obtained by chemical oxidative reaction of the corresponding high temperature phases [17]. Removal of Cu from the β- and ϵ-Cu–V–O phases is done by stirring the materials in a solution of acetonitrile or CCl_4 containing an oxidizing agent (Br_2, NO^+, NO_2^+) at room temperature or at 80 °C. In this way, new β-copper vanadium bronzes β-$Cu_yV_2O_5$ $(0<y<0.26)$ are obtained. Electrochemical Li insertion (for $y=0.006$) results in a cell capacity of ≈ 260 Ah/kg, similar to that obtained with β-$Na_{0.33}V_2O_5$. The best results are reported when chemical partial removal of Cu is performed from the layered ϵ-$Cu_{0.85}V_2O_5$ phase to give ϵ-$Cu_{0.2}V_2O_5$. In this case, Li cells using this new compound and operating between 4 and 2 V can develop a maximum specific capacity of 380 Ah/kg which corresponds to the reversible insertion of ≈ 2.4 Li^+ per mole of bronze. The cycling properties of the material are excellent since the massic capacity decreases only 15% after 50 cycles. Similar studies have been also extended to δ-$Ag_yV_2O_5$ phases.

2.3.2. Ion-exchange reactions

Exchange reactions must be considered with interest for preparing cathodic materials. Chemical extraction of Li ions from the Li_2MnO_3 rock-salt structure [18] results in a topotactic exchange reaction. H^+/Li^+ exchange process is performed in HCl solution at 80 °C, and protons are eliminated from the structure by a further thermolysis at 300 °C. Under these conditions, up to one Li^+ ion can be removed, without destroying the host structure leading to compounds with cationic vacancies ($Li_{1.34}Mn_{1.16}O_3$, $LiMn_{1.25}O_3$). Only one reduction process is pointed out near 3 V, corresponding to the reversible insertion of 0.4 to 0.6 Li ions. Cycling experiments have been performed in button cells in the potential range from 4 to 2 V. The initial capacity slowly diminishes with the cycles number to reach a value of nearly 100 Ah/kg after the 20th cycle.

Recently, a new synthesis route based on Li-ion exchange involving γ-MnOOH in a concentrated lithium hydroxyde aqueous solution at 100 °C leads to the formation of an orthorhombic LT $LiMnO_2$ [19] (Fig. 4). An irreversible structural change takes place during the first charge cycle at higher voltage than all subsequent cycles. The new phase reported to be a disordered spinel when Li is removed from $LiMnO_2$, exhibits a good cycling behaviour in the 3.8–2 and 4.2–2 V voltage range with a specific capacity of 120 and 180 Ah/kg, respectively. This work constitutes an interesting result in regard to $LiMn_2O_4$ characterized by a low specific capacity of 110 Ah/kg and in comparison with the HT $LiMnO_2$ which has poor reversible capacity.

2.3.3. Electrochemical preparation

Interest has been recently emphasized on electrolytic V_2O_5 obtained by constant potential electrolysis of a

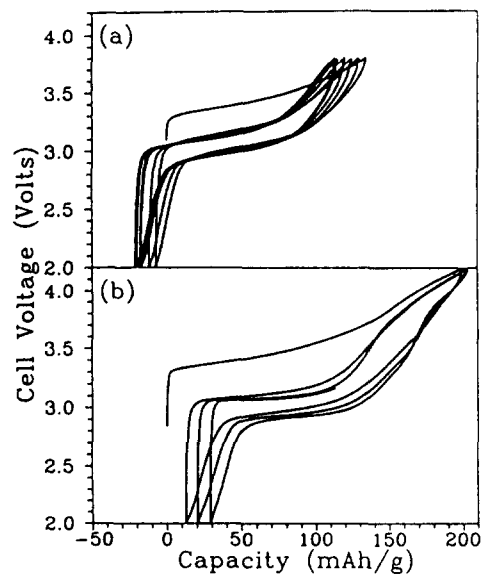

Fig. 4. Cycling behaviour of LT $LiMnO_2$ synthesized via ion-exchange procedure. (a) 3.8–2 V; (b) 4.2–2 V; 5.7 mA/g; from Ref. [19].

V(IV) aqueous solution [20]. The deposit dried at 110 °C in vacuum leads to a quasi-amorphous phase. Compared with the behaviour of the classical amorphous V_2O_5, crystalline V_2O_5, and V_2O_5–P_2O_5 electrodes, the discharge profile of this material shows the highest discharge voltage with one loose step at about 2.7 V, the greatest discharge capacity (230 Ah/kg) at a cutoff voltage of 2 V and a good cycleability between 3.5 and 2 V while its specific capacity is about 150 Ah/kg, a few percent larger than that of V_2O_5–P_2O_5.

Thermal decomposition of $(NH_4)_xK_{4-x}V_6O_{16+y}$, $0 \leqslant x \leqslant 4$ and $0 \leqslant y \leqslant 0.1$ deposited on nickel substrates by cyclic voltammetry under air or inert atmospheres at 350 °C results in the formation of adherent crystalline $K_xV_6O_{13+y}$ without the use of binders, $0 \leqslant x \leqslant 3.7$ and $0.1 \leqslant y \leqslant 3.1$ [21]. Their discharge capacity for Li insertion strongly depends on the K/V and O/V ratios. The best results are obtained for K/V = 0.2 and O/V = 2.6; about 4.5 Li^+ ions enter reversibly $K_{1.2}V_6O_{15.6}$ with a discharge curve intermediate between those of V_2O_5 and V_6O_{13} in the 3.5–1.5 V potential range. In a similar way, a new potassium bronze $K_{1.2}V_6O_{13.8}$ can be synthesized and has been proved to be suitable for use in a rechargeable Li cell with an initial discharge capacity of 0.7 F/V.

All these results emphasize the interest in the 'low-temperature techniques' over solid-state reactions in obtaining new and high performance cathodic materials for secondary Li batteries. Further works in this area should allow to provide significant advances in the field of Li batteries.

Acknowledgements

The author would like to thank Professor N. Baffier (CNRS URA 1466), Dr J. Farcy and Dr S. Bach (CNRS UM 28) for their helpful discussions. The financial support by the 'Direction des Recherches, Etudes et Techniques' (DRET) and the 'Centre National d'Etudes Spatiales' (CNES) is gratefully acknowledged.

References

[1] J.P. Pereira-Ramos, N. Baffier and G. Pistoia, in G. Pistoia (ed.), *Lithium Batteries*, Elsevier, Amsterdam, 1994, p. 281.
[2] K. West, B. Zachau-Christiansen, M.J.L. Ostergard and T. Jacobsen, *J. Power Sources, 20* (1987) 165.
[3] M.G. Minett and J.R. Owen, *J. Power Sources, 32* (1990) 81.
[4] S. Maingot, R. Baddour, J.P. Pereira-Ramos, N. Baffier and P. Willmann, *J. Electrochem. Soc., 140* (1993) L158.
[5] S. Maingot, Ph. Deniard, N. Baffier, J.P. Pereira-Ramos, A. Kahn-Harrari and R. Brec, *J. Power Sources*, submitted for publication.
[6] P. Legoff, N. Baffier, S. Bach and J.P. Pereira-Ramos, *J. Mater. Chem., 4* (1994) 875.
[7] S. Bach, J.P. Pereira-Ramos, C. Cachet and L.T. Yu, *Electrochim. Acta*, in press.
[8] P. Barboux, J.M. Tarascon and F.K. Shokoohi, *J. Solid State Chem., 94* (1991) 185.
[9] G. Pistoia, M. Pasquali, G. Wang and L. Li, *J. Electrochem. Soc., 137* (1990) 2365.
[10] M. Pasquali and G. Pistoia, *Electrochim. Acta, 36* (1991) 1549.
[11] J. Farcy, J.P. Pereira-Ramos, L. Hernan, J. Morales and J.L. Tirado, *Electrochim. Acta, 39* (1994) 339.
[12] B. Garcia, J. Farcy, J.P. Pereira-Ramos, N. Baffier and J. Perichon, *J. Power Sources*, submitted for publication.
[13] M. Yoshio, H. Tanaka, K. Tominaga and H. Noguchi, *J. Power Sources, 40* (1992) 347.
[14] N. Kumagai, Y. Matsuura, N. Kumagai and K. Tanno, *J. Electrochem. Soc., 139* (1992) 3553.
[15] M. Sugawara, Y. Kitada and K. Matsuki, *J. Power Sources, 26* (1989) 373.
[16] R.J. Gummow and M.M. Thackeray, *J. Electrochem. Soc., 140* (1993) 3365.
[17] F. Garcia-Alvarado and J.M. Tarascon, *Solid State Ionics, 63–65* (1993) 401.
[18] F. Lubin, A. Lecerf, M. Broussely and J. Labat, *J. Power Sources, 34* (1991) 161.
[19] J.N. Reimers, E.W. Fuller, E. Rossen and J.R. Dahn, *J. Electrochem. Soc., 140* (1993) 3396.
[20] Y. Sato, T. Nomura, H. Tanaka and K. Kobayakawa, *J. Electrochem. Soc., 138* (1991) L37.
[21] E. Andrukaitis, *J. Power Sources, 43/44* (1993) 603.